Vietnam Journal of Science and Technology
DOI: https://doi.org/10.15625/2525-2518/24045

In silico and *in vitro* investigation of curcuminoid as potential TLR4/MD-2 complex inhibitors using molecular docking and molecular dynamic simulations

Dinh Thi Tu[1,2], Ngo Kim Chi[1], Le Thi Thuy Huong[1,2], Do Huu Nghi[1], Pham Minh Quan[1,2,*]

[*]Email: *pham-minh.quan@ich.vast.vn*

Received: 02 January 2026; Accepted for publication: 15 February 2026

Abstract. Inflammation is a key pathological process in many chronic diseases, in which the Toll-like receptor 4/myeloid differentiation factor-2 (TLR4/MD-2) complex serves as a critical upstream regulator. Curcuminoids, naturally occurring polyphenols abundant in *Curcuma* species cultivated in Vietnam, possess well-documented anti-inflammatory properties; however, their molecular interactions with TLR4/MD-2 remain poorly understood. In this study, an integrated *in silico* and *in vitro* strategy was employed to evaluate the anti-inflammatory potential of three major curcuminoids: curcumin, demethoxycurcumin, and bisdemethoxycurcumin. Molecular docking indicated that curcumin and bisdemethoxycurcumin exhibited strong binding affinities toward the TLR4/MD-2 complex, with docking scores of -9.29 and -9.73 kcal/mol, respectively. Molecular dynamic simulations further confirmed the structural stability of these complexes and revealed persistent key interactions. ADMET predictions suggested favorable drug-likeness and low toxicity profiles. Consistently, *in vitro* assays using LPS-stimulated RAW 264.7 macrophages demonstrated that curcumin and bisdemethoxycurcumin significantly inhibited nitric oxide production, with IC_{50} values of 121.06 ± 2.16 µg/mL and 91.22 ± 1.58 µg/mL, whereas demethoxycurcumin showed negligible activity. Overall, curcumin and bisdemethoxycurcumin emerge as promising natural compounds for the development of TLR4/MD-2-targeted anti-inflammatory agents.

Keywords: curcuminoid, anti-inflammatory, molecular docking, molecular dynamic, TLR4/MD-2.

Classification numbers: 1.2.1, 1.2.4.

1. INTRODUCTION

Inflammation is a fundamental biological response of the innate immune system to infection, tissue injury, and various endogenous danger signals; however, dysregulated or excessive inflammatory responses are implicated in the pathogenesis of numerous chronic diseases, including rheumatoid arthritis, inflammatory bowel disease, neurodegenerative disorders, and cancer [1, 2]. Among the key molecular regulators of inflammatory signaling, Toll-like receptor 4 (TLR4) and its co-receptor myeloid differentiation factor-2 (MD-2) play a pivotal role in initiating innate immune responses [3]. The TLR4/MD-2 complex recognizes pathogen-associated molecular patterns, most notably lipopolysaccharide (LPS), leading to receptor dimerization and activation of downstream signaling cascades such as nuclear factor-

κB (NF-κB) and mitogen-activated protein kinase (MAPK) pathways [4]. This activation results in the transcriptional upregulation of pro-inflammatory mediators, including tumor necrosis factor-α, interleukins, cyclooxygenase-2, and inducible nitric oxide synthase [5]. Owing to its upstream position in the inflammatory cascade and its capacity to regulate multiple pro-inflammatory pathways simultaneously, the TLR4/MD-2 complex has emerged as an attractive and strategically important therapeutic target for the development of anti-inflammatory agents. Inhibiting TLR4/MD-2 signaling offers the potential to modulate excessive inflammatory responses at an early stage, thereby providing broader and more effective anti-inflammatory outcomes compared to targeting individual downstream mediators. Most currently available anti-inflammatory drugs, despite their proven therapeutic efficacy, are associated with a range of adverse effects that limit their long-term clinical use [6, 7]. These side effects include hepatotoxicity, gastrointestinal complications, increased risks of cardiovascular events, renal impairment, and hypertension. Consequently, there is a growing demand for the development of next-generation anti-inflammatory agents that retain strong anti-inflammatory efficacy while exhibiting improved safety profiles and reduced systemic toxicity.

Curcuminoids are a prominent class of naturally occurring polyphenolic compounds predominantly found in the rhizomes of *Curcuma* species, which are widely cultivated and traditionally used in Vietnam. The major curcuminoids including curcumin (curcumin I), demethoxycurcumin (curcumin II) and bisdemethoxycurcumin (curcumin III), exhibit considerable structural diversity arising from variations in methoxy substitution patterns on the aromatic rings, which in turn influence their physicochemical properties and biological activities. Previous studies have demonstrated a broad spectrum of biological activities of curcuminoids, including antioxidant, anticancer, antimicrobial, and neuroprotective effects. Notably, curcuminoids have been reported to exert anti-inflammatory effects through the modulation of multiple signaling pathways, such as nuclear factor-κB, mitogen-activated protein kinases, and the expression of pro-inflammatory mediators [8, 9]. However, despite these well-documented activities, the precise molecular mechanisms underlying their interactions with upstream inflammatory targets remain incompletely understood. In particular, the differential roles and structure–activity relationships of individual curcuminoids in regulating key innate immune receptors have not been fully elucidated, highlighting a significant and largely unexplored potential for curcuminoids in the rational development of novel anti-inflammatory agents.

In recent years, computational drug discovery approaches have become powerful tools for the identification of new therapeutic candidates and for gaining insights into the molecular mechanisms governing the biological effects of bioactive compounds. In the present study, an integrated in silico strategy combining molecular docking and pharmacokinetic prediction was applied to investigate the anti-inflammatory potential of curcuminoids targeting the Toll-like receptor 4/myeloid differentiation factor-2 (TLR4/MD-2) complex. In parallel, the anti-inflammatory activities of different curcuminoid forms were experimentally assessed through nitric oxide (NO) production inhibition assays, allowing a direct comparison between the computational predictions and biological outcomes. Subsequently, the drug-likeness and absorption, distribution, metabolism, excretion, and toxicity (ADMET) profiles of the investigated compounds were evaluated to identify candidates with favorable pharmacokinetic characteristics. The final selection of promising anti-inflammatory candidates was therefore based on the combined evaluation of predicted binding potency toward the TLR4/MD-2 complex, pharmacokinetic suitability, and consistency with NO inhibition activity.

2. MATERIALS AND METHODS

2.1. Ligand and protein preparation

The structural modeling of the curcuminoids was initiated by generating 2D and 3D geometries via MarvinSketch (v19.27.0) and PyMOL (v1.3.r1) (Figure 1) [10]. To refine these structures, energy minimization was executed using Gabedit (v2.5.0) [11]. Given the use of RAW264.7 cell lines in the experimental phase, the docking simulations focused on the murine TLR4/MD-2 complex. The corresponding X-ray crystal structures were retrieved from the RCSB Protein Data Bank under the identifiers 2Z64 and 3VQ2. Both models fall within the high-quality resolution range of 1.5–3.0 Å required for precise docking. Initially, the monomeric, LPS-free form (2Z64) was utilized to delineate the putative binding site in its inactive state. Subsequently, the dimeric active conformation (3VQ2), characterized by the presence of LPS, was employed to validate the binding orientations and confirm the inhibitory potential of the studied compounds.

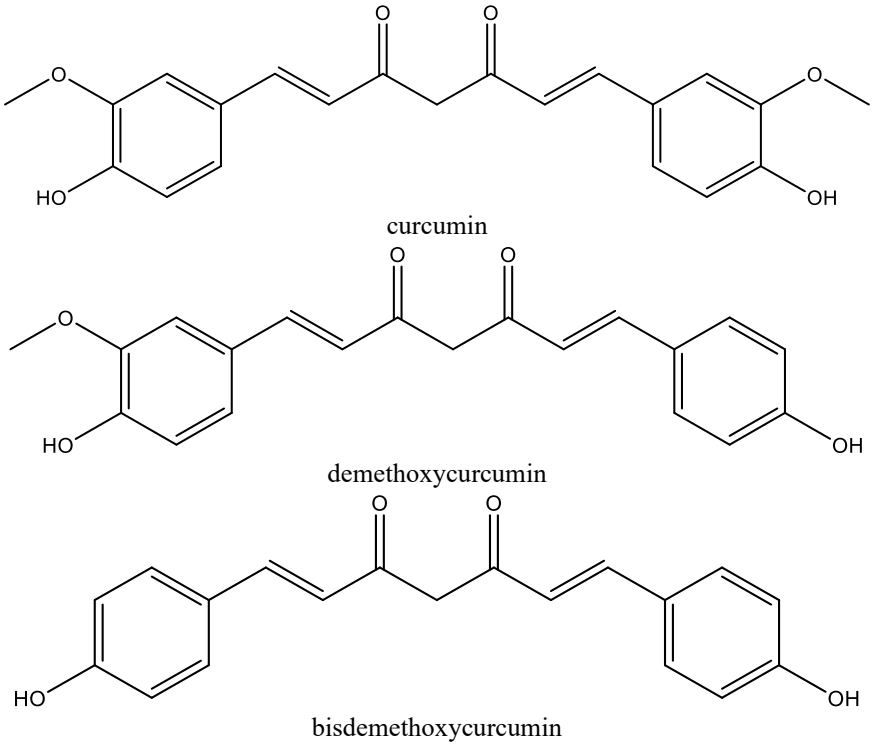

Figure 1. Structure of curcumin, demethoxycurcumin and bisdemethoxycurcumin.

2.2. Docking using Autodock

The preparation of both macromolecules and ligands was conducted through AutoDock Tools v1.5.6rc3 (ADT) [12]. The receptor was refined by eliminating crystallographic water molecules to generate a desolvated structure. Subsequently, polar hydrogen atoms, solvation parameters, and Kollman partial charges were assigned to the protein. To define the search space, a grid box was strategically centered to encapsulate the known binding domains of validated reference ligands. Molecular docking was executed using the Lamarckian Genetic Algorithm (LGA) within AutoDock 4.2. AutoDock was run by using autodock parameters as

follows: GA population size, 300; maximum number of energy evaluations, 25 000 000; and the number of generations, 27 000. A maximum of 50 conformers were considered for each molecule, and the root-mean-square (RMS) cluster tolerance was set to 2.0 Å in each run. Following the simulations, the conformation exhibiting the minimum binding free energy from the most populated cluster was prioritized for downstream evaluation. Post-docking visualization and interaction mapping were performed using PyMOL and Discovery Studio Visualizer.

2.3. Molecular dynamic simulation

To investigate the binding behavior of tyrosinase with various inhibitors, MD simulations were conducted via GROMACS. The simulation setup utilized a combination of Amber99SB-iLDN, TIP3P, and GAFF for the protein, solvent, and inhibitors, respectively. For the ligands, structural data were refined using DFT calculations (B3LYP/6-31G(d,p)), and charges were derived using the RESP method within an implicit solvent ($\varepsilon = 78.4$). The complex was solvated in a 6.3 × 6.3 × 6.3 nm dodecahedron box, resulting in a total system size of roughly 28,000 atoms. The protocol involved a rigorous equilibration process, including steepest descent minimization followed by NVT and NPT ensembles. A 50 ns production phase was initiated from the final NPT coordinates, during which C_α backbone restraints were maintained. The entire simulation workflow was replicated three times to ensure the statistical significance and thorough sampling of the results.

2.4. ADMET studies

The pharmacokinetic profiles and safety margins of the investigated molecules were assessed using a multi-platform *in silico* approach. The Molinspiration [13] and ProTox-II web servers were employed to predict drug-likeness parameters and acute toxicity levels, respectively. Furthermore, comprehensive ADMET descriptors - including absorption, distribution, metabolism, excretion, and toxicity - were calculated using the admetSAR database [14]. These simulations provided a predictive framework for evaluating the biological viability and metabolic fate of the research compounds.

2.5. *In vitro* anti-inflammatory assay

Curcuminoids (Curcumin I, II and III) samples were provided by Dr. Do Tien Lam, Department of Agricultural Biochemistry and Essential Oils, Institute of Chemistry, Vietnam Academy of Science and Technology. The anti-inflammatory activity of the extracts and isolated compounds was determined through the inhibition of nitrite oxide (NO) production in lipopolysaccharide (LPS)-induced RAW264.7 cells (ATCC, Manassas, VA, USA) according to procedures previously described [15]. All data are presented as means of three replicates ± standard deviations. A mouse macrophage cell line RAW 264.7 was purchased from the American Type Culture Collection (Manassas, VA, USA) and maintained in DMEM supplemented with 10 % fetal bovine serum (FBS; HyClone, GE Healthcare, UT, USA) and 1 % penicillin-streptomycin at 37 °C in a 5 % CO_2 incubator.

The suppressive effect of the investigated compounds on nitric oxide (NO) production was quantified using lipopolysaccharide (LPS)-activated RAW 264.7 murine macrophages. Initially, cells were plated in 96-well scaffolds at a density of 2×10^5 cells per well and maintained under standard physiological conditions 37 °C and 5 % CO_2 for 24 h. Stock solutions of the test

candidates were prepared in 100% DMSO (20 mM) and subsequently subjected to four concentration ranges from high to low in serum-free DMEM. Following a 2-hour pretreatment with the varying concentrations, NO secretion was induced by the addition of LPS (10 mg/ml) for an incubation period of 24 h. Cardamonin served as the reference anti-inflammatory agent (100; 20; 4 and 0.8 mM), while cells treated with the vehicle alone acted as negative controls. The accumulation of nitrite (NO_2^-) in the culture supernatant, a surrogate marker for NO synthesis, was measured via the Griess Reagent System (Promega, WI, USA). Briefly, 100 ml of the conditioned medium was combined with an equal volume of Griess reagent 0 consisting of 1 % sulfanilamide (in 5 % phosphoric acid) and 0.1 % N-1-naphthylethylenediamine dihydrochloride. After a 10-minute incubation at ambient temperature, the optical density was recorded at 540 nm using a spectrophotometric microplate reader. Nitrite concentrations were extrapolated from a $NaNO_2$ standard curve, and the results were expressed as a percentage of the LPS-stimulated control. The inhibitory potency of each sample was calculated using the following equation:

$$(\%)\ \text{inhibition} = 100\ \% - [\text{content } NO_{sample}/\text{content NOLPS}] \times 100$$

Cardamonin, a well-known anti-inflammatory agent, was used as positive control. To ensure the reproducibility and statistical reliability of the findings, all experimental assays were performed in triplicate. The half-maximal inhibitory concentration (IC_{50}), representing the dosage required to suppress nitric oxide (NO) production by 50 % relative to the stimulated control, was calculated through non-linear regression analysis. This quantification was executed using the specialized curve-fitting software TableCurve 2D v4.0.

2.6. Statistical analysis

The docking results obtained from AutoDock were further examined using PyMOL and Discovery Studio Visualizer. PyMOL was employed to measure hydrogen bond lengths by calculating the distance between hydrogen atoms and their corresponding interaction partners. Hydrogen bonds were considered present when the acceptor–hydrogen–donor (A–H–D) angle exceeded 135° and the distance between the acceptor and donor atoms was less than 0.35 nm. The protonation states of the ligands were assigned using the Chemicalize web platform developed by ChemAxon. In addition, structural stability was evaluated by calculating the root-mean-square deviation (RMSD) of atomic coordinates using the “gmx rms” module implemented in GROMACS.

3. RESULTS AND DISCUSSION

3.1. Molecular docking studies

Given that the *in vitro* assays in this study were performed using RAW264.7 macrophages, molecular docking analyses were conducted to elucidate the putative interactions between curcuminoids and the TLR4/MD-2 complex. AutoDock4, a well-established and extensively cited molecular docking platform, was selected due to its reliability in estimating ligand–target binding affinities and docking conformations. In the present work, AutoDock4 was employed to investigate the possible binding mechanisms of the bioactive curcuminoids, and the corresponding docking scores are presented in Table 1.

Table 1. Dock score and key residue interactions of curcuminoids with TLR4/MD-2 complex.

Compounds	Dock score (kcal/mol)	H-bond interacting residues (preMD)	H-bond interacting residues (MD refined)
curcumin I	-9.29	Lys263	Asp101, Lys263, Phe406
curcumin II	-7.53	Arg337, Arg380, Ala382	-
curcumin III	-9.73	Gly315	Arg337, Asn359

Based on the scoring scheme implemented in AutoDock4, more negative docking energy values are indicative of stronger ligand–receptor interactions. The docking analysis revealed that curcumin I and curcumin III exhibited favorable binding toward the target protein, with predicted binding energies of -9.29 and -9.73 kcal/mol, respectively. The stereoview binding orientations of these ligands within the active site are illustrated in Figure 1.

(A)

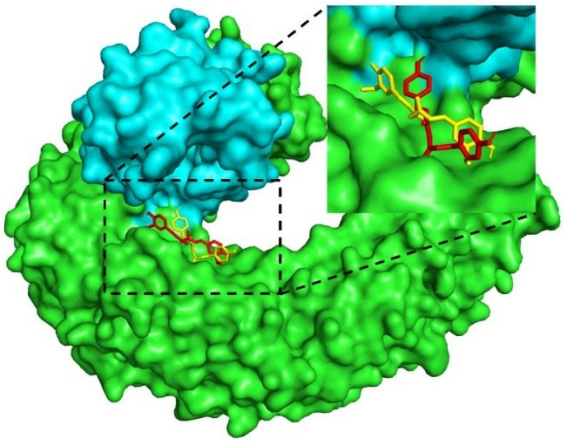

(B)

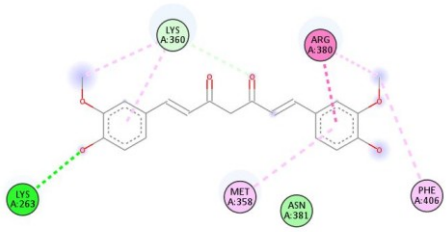

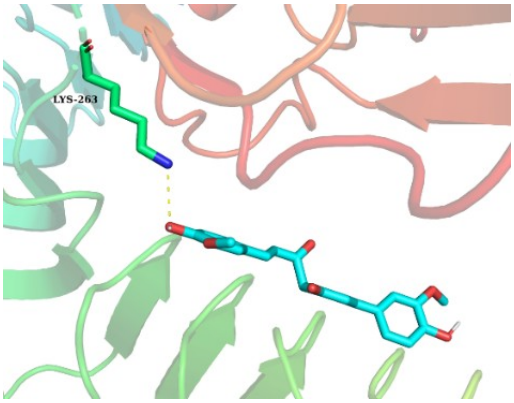

(C)

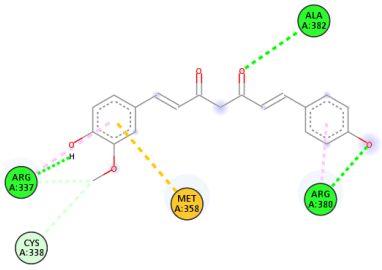

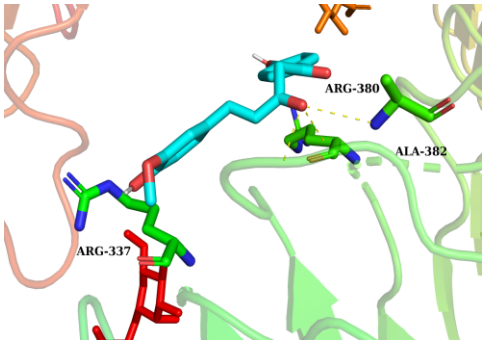

(D)

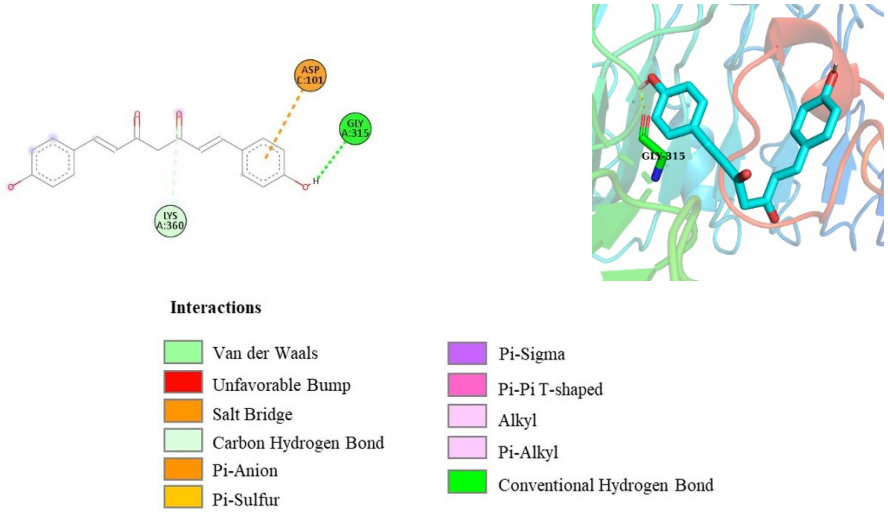

Figure 1. Interaction between curcumin I and curcumin III in the complex with TLR4/MD-2 obtained via AutoDock4 docking package. (A) Studied compounds bind to a smooth region in TLR4, adjacent to its contact interface with MD-2: curcumin I-red, curcumin III-yellow; (B) Dock pose of curcumin I; (C) Dock pose of curcumin II; (D) Dock pose of curcumin III.

Obtained results indicated that curcumin I docked to TLR4/MD-2 through one hydrogen bond with Lys263, an array of hydrophobic contact was contributed by Met358, Lys360, Arg380, Asn381, Phe406. On the other hand, curcumin III was obserbed to form one H-bond with Gly315 and the interaction was further strengthen by weak contact with Asp101 and Lys360.

3.2. Molecular dynamic studies

While molecular docking serves as an efficient tool for virtual screening, its reliance on a static receptor framework and implicit solvation often limits the accuracy of its predictions. To overcome these constraints - such as the lack of conformational flexibility and receptor dynamics - molecular dynamic (MD) simulations were implemented to further refine the docking poses. Each enzyme-inhibitor complex underwent a 50 ns MD production run, initiated from the primary docked configurations, to facilitate structural relaxation in an aqueous environment. As depicted in Figure 2, the trajectory analysis confirmed that all systems attained thermodynamic equilibrium within the first 10 ns. The stability of these complexes was evidenced by minimal Root Mean Square Deviation (RMSD) fluctuations, which remained consistently around 0.2 nm for the duration of the study.

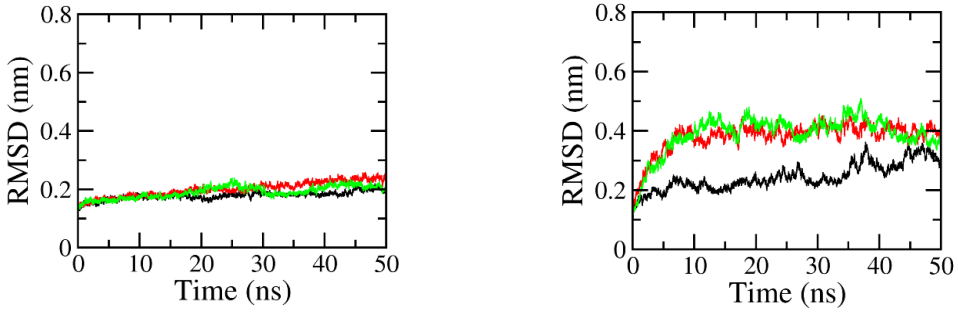

Figure 2. All-atoms RMSD of TLR4/MD-2 with curcumin I (A) and curcumin III (B) over 3 independent MD simulations of 50 ns.

The observed stability indicates that ligand binding induced no substantial conformational disturbances, thus maintaining the structural integrity of the TLR4/MD-2 complex throughout the simulation period. The representative dock poses of curcumin I and curcumin III within the TLR4/MD-2 binding site are displayed in Figure 3.

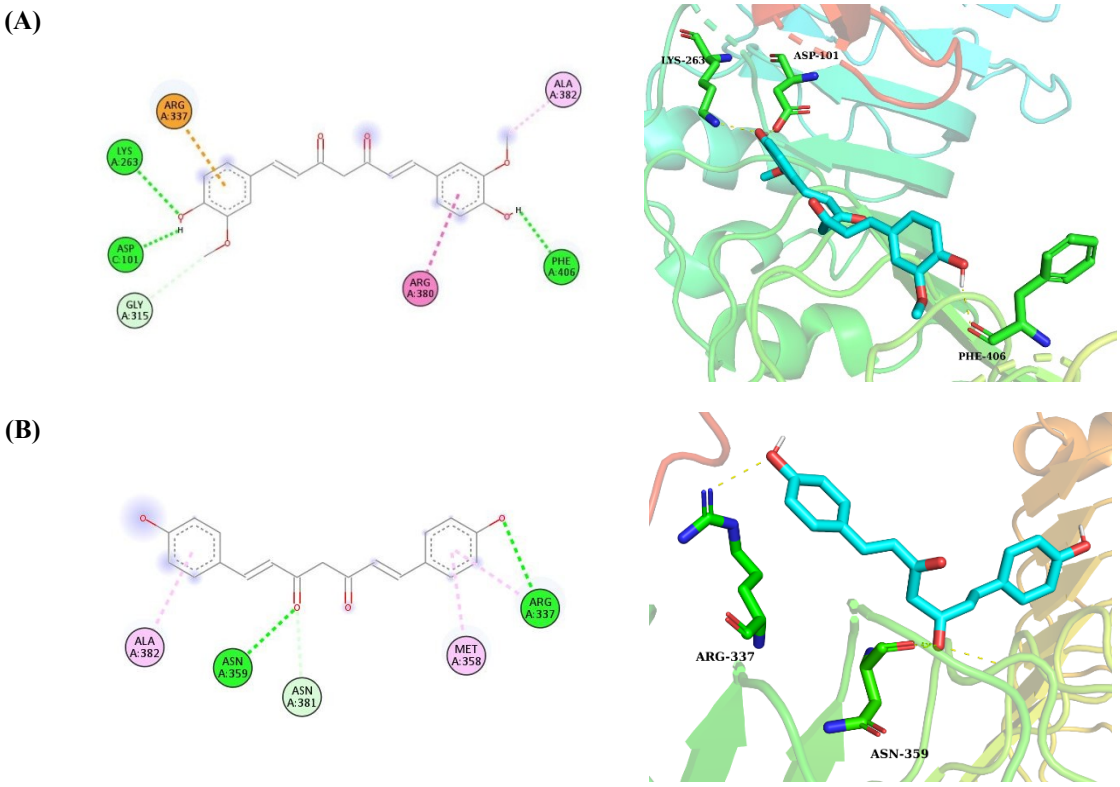

Figure 3. MD refined structure binding pose between curcumin I (A) and curcumin III (B) to TLR4/MD-2, which was obtained via clustering method over equilibrium snapshots of the complex with a cutoff of 0.2 nm.

The interaction analysis revealed that curcumin I formed three conventional hydrogen bonds with the target protein, involving residues Asp101, Lys263, and Phe406. The

hydrophobic pockets formed with this ligand involving residues Gly315, Arg337, Arg380, Ala382. Binding conformation analysis of curcumin III indicate that the hydrogen bonds were constituted from interaction with Arg337 and Asn359 while hydrophobic interactions were primarily mediated by residues Asn381, Ala382, and Met358.

3.3. ADMET profile

The drug-likeness of the two selected candidates was initially evaluated in accordance with Lipinski's Rule of Five (Ro5), a widely accepted criteria for predicting oral bioavailability [16]. The two potential curcuminoids were subsequently subjected to *in silico* assessment of pharmacokinetic behavior and toxicity potential using the Molinspiration and ProTox 3.0 webservers, the results are summarized in Table 2.

Table 2. ADMET properties and toxicity prediction of potential inhibitors.

CP	MW	HBD	HBA	LogP	MR (cm^3/mol)	TPSA ($Å^2$)[a]	LD_{50} (mg/kg)	Toxicity prediction[b]	HIA (%)
curcumin I	368	2	6	3.72	102.80	93.06	2000	4	93.30
curcumin III	308	2	4	3.24	89.82	74.60	2560	5	94.20

[a] Molecular total polar surface area.

[b] Toxicity prediction class: 1 → 6 (High toxicity to non-toxic).

Both curcumin I and III exhibit favorable physicochemical profiles for oral administration, strictly adhering to Lipinski's Rule of Five with zero violations. Results from pharmacokinetic modeling and docking simulations consistent with the high-precision scoring of AutoDock4 thus, indicate that these natural derivatives are potent TLR4/MD-2 inhibitors with significant drug-like potential. Furthermore, their classification into toxicity categories 4 and 5, alongside favorable LD_{50} estimates, underscores a safety margin that supports their futher drug development.

3.4. Anti-inflammatory activity

Curcuminoids were screened for anti-inflammatory activity using an LPS-induced RAW 264.7 macrophage model to monitor NO production inhibition. The corresponding *in vitro* results are documented in Table 3.

Table 3. Inhibitory ability of NO production of curcuminoids.

No	Compound name	IC_{50} (µg/mL)
1	curcumin I	121.06 ± 2.16
2	curcumin II	> 200
3	curcumin III	91.22 ± 1.58
	cardamonin	0.61 ± 0.24

The IC_{50} value data of the compounds in Table 3 showed that curcumin I and curcumin III exhibited potent anti-inflammatory activity compared to the positive control drug cardamonin (IC_{50} = 0.61 µg/mL) with IC_{50} values of 121.06 µg/mL and 91.22 µg/mL, respectively. These results show a correlation with data obtained from *in silico* studies.

4. CONCLUSIONS

In this study, an integrated *in silico–in vitro* approach was employed to investigate the anti-inflammatory potential of major curcuminoids targeting the TLR4/MD-2 complex, a critical upstream regulator of innate immune responses. Molecular docking and molecular dynamic simulations suggested that curcumin and especially bisdemethoxycurcumin bind stably to the TLR4/MD-2 complex through persistent hydrogen bonding and hydrophobic interactions with key residues involved in receptor activation. Among the investigated compounds, bisdemethoxycurcumin exhibited the most favorable binding affinity and maintained a highly stable binding conformation during molecular dynamic simulations, indicating a strong and sustained interaction with the target protein complex. Pharmacokinetic and toxicity predictions further revealed that bisdemethoxycurcumin complies with Lipinski's rule of five, shows high predicted intestinal absorption, and possesses a low toxicity profile, supporting its suitability as a drug-like molecule. Consistently, *in vitro* evaluation using LPS-stimulated RAW 264.7 macrophages confirmed that bisdemethoxycurcumin more effectively inhibited nitric oxide production than curcumin, in agreement with the *in silico* results. The molecular docking results also provided a preliminary prediction of the anti-inflammatory mechanism of action at the molecular level, offering a robust structural basis for understanding how these compounds modulate innate immune signaling. Collectively, these findings identify bisdemethoxycurcumin as the most promising curcuminoid among those studied and highlight its potential as a natural lead scaffold for the development of novel anti-inflammatory agents targeting the TLR4/MD-2 signaling pathway.

Declaration of competing interest. The authors declare that they have no known competing financial interests or personal relationships that could have appeared to influence the work reported in this paper.

REFERENCES

1. Nguyen T. T. T., Tran V. A., Tran T. H., Ho V. D., Do T. H., Truong Q. K., Pham M. Q., Le T. H. V. - Megastigmanes isolated from *Boehmeria nivea* leaves and their immunomodulatory effect on IL-1β and IL-10 production in RAW264.7 macrophages. RSC Adv., **15**(15) (2025) 11549-11561. https://doi.org/10.1039/d4ra06545j.
2. Rahman S. U., Li Y., Huang Y., Zhu L., Feng S., Wu J., Wang X. - Treatment of inflammatory bowel disease via green tea polyphenols: possible application and protective approaches. Inflammopharmacology, **26**(2) (2018) 319-330. https://doi.org/10.1007/s10787-018-0462-4.
3. Hsu C. L., Fang S. C., Yen G. C. - Anti-inflammatory effects of phenolic compounds isolated from the flowers of *Nymphaea mexicana* Zucc. Food Funct., **4**(8) (2013) 1216-1222. https://doi.org/10.1039/c3fo60041f.
4. Bauer M. E., Teixeira A. L. - Inflammation in psychiatric disorders: what comes first? Ann. N.Y. Acad. Sci., **1437**(1) (2018) 57-67. https://doi.org/10.1111/nyas.13712.
5. Balahura Stamat L. R., Dinescu S. - Inhibition of NLRP3 inflammasome contributes to paclitaxel efficacy in triple negative breast cancer treatment. Sci. Rep., **14**(1) (2024) 24753. https://doi.org/10.1038/s41598-024-75805-3.
6. Sharma S., Kumar D., Singh G., Monga V., Kumar B. - Recent advancements in the development of heterocyclic anti-inflammatory agents. Eur. J. Med. Chem., **200** (2020) 112438. https://doi.org/10.1016/j.ejmech.2020.112438.
7. Bian M., Ma Q. Q., Wu Y., Du H. H., Guo-Hua G. - Small molecule compounds with good anti-inflammatory activity reported in the literature from 01/2009 to 05/2021: a review. J.

Enzyme Inhib. Med. Chem., **36**(1) (2021) 2139-2159. https://doi.org/10.1080/14756366.2021.1984903.

8. Kasetsuwan N., Reinprayoon U., Uthaithammarat L., Sereemaspun A., Sae-Liang N., Chaichompoo W., Suksamrarn A. - Anti-inflammatory effect of curcuminoids and their analogs in hyperosmotic human corneal limbus epithelial cells. BMC Complement Med Ther, **24**(1) (2024) 172. https://doi.org/10.1186/s12906-024-04448-8.
9. Sandur S. K., Pandey M. K., Sung B., Ahn K. S., Murakami A., Sethi G., Limtrakul P., Badmaev V., Aggarwal B. B. - Curcumin, demethoxycurcumin, bisdemethoxycurcumin, tetrahydrocurcumin and turmerones differentially regulate anti-inflammatory and anti-proliferative responses through a ROS-independent mechanism. Carcinogenesis, **28**(8) (2007) 1765-1773. https://doi.org/10.1093/carcin/bgm123.
10. Schrodinger L. L. C. - The PyMOL Molecular Graphics System, Version 1.3r1.(2010).
11. Allouche A. R. - Gabedit-A graphical user interface for computational chemistry softwares. J. Comput. Chem., **32**(1) (2011) 174-182. https://doi.org/10.1002/jcc.21600.
12. Morris G. M., Huey R., Lindstrom W., Sanner M. F., Belew R. K., Goodsell D. S., Olson A. J. - AutoDock4 and AutoDockTools4: Automated docking with selective receptor flexibility. J. Comput. Chem., **30**(16) (2009) 2785-2791. https://doi.org/10.1002/jcc.21256.
13. Molinspiration Cheminformatics FreeWeb Services - Slovensky Grob, Slovakia. https://www.molinspiration.com/cgi-bin/properties (accessed 16 December 2025).
14. Cheng F., Li W., Zhou Y., Shen J., Wu Z., Liu G., Lee P. W., Tang Y. - admetSAR: A comprehensive source and free tool for assessment of chemical ADMET properties. J. Chem. Inf. Model., **52**(11) (2012) 3099-3105. https://doi.org/10.1021/ci300367a.
15. Cheenpracha S., Park E. J., Rostama B., Pezzuto J. M., Chang L. C. - Inhibition of Nitric oxide (NO) production in lipopolysaccharide (LPS)-Activated murine macrophage RAW 264.7 cells by the norsesterterpene peroxide, epimuqubilin A. Mar. Drugs, **8**(3) (2010) 429-437. https://doi.org/10.3390/md8030429.
16. Lipinski C. A. - Drug-like properties and the causes of poor solubility and poor permeability. J. Pharmacol Toxicol Methods, **44**(1) (2000) 235-249. https://doi.org/10.1016/s1056-8719(00)00107-6.